



Continuous In Situ Measurement of Dissolved Methane in Lake Kivu Using a Membrane Inlet Laser Spectrometer

Roberto Grilli¹, François Darchambeau², Jérôme Chappellaz¹, Ange Mugisha³, Jack Triest⁴ and Augusta Umutoni³

5 ¹ CNRS, Univ. Grenoble Alpes, IRD, Grenoble INP, IGE, F-38000 Grenoble, France

² KivuWatt Ltd., Kigali, Rwanda and Chemical Oceanography Unit, Université de Liège, Belgium

³ Lake Kivu Management Program LKMP, Gisenyi, Rwanda

⁴ KM Contros, Kongsberg Maritime, Kiel, Germany

Correspondence to: Roberto Grilli (roberto.grilli@cnrs.fr)

10 **Abstract.** We report the first high resolution continuous profile of dissolved methane in the shallow water of Lake Kivu, Rwanda. The measurements were performed using an in situ dissolved gas sensor, called Sub-Ocean, based on a patented, membrane based extraction technique coupled with a highly sensitive optical spectrometer. The sensor was originally designed for ocean settings, but both the spectrometer and the extraction system were modified to extend the dynamical range up to six orders of magnitude with respect to the original prototype (from nmol L^{-1} to mmol L^{-1} detection) to fit the range of
15 concentrations at lake Kivu. The accuracy of the instrument was estimated to $\pm 22\%$ (2σ) from the standard deviation of eight profiles at 80 m of depth, corresponding to $\pm 112 \mu\text{Bar}$ of CH_4 in water or $\pm 160 \text{ nmol L}^{-1}$ at 25°C and 1 atm. The instrument was able to continuously measure the top 150 m of water depth within only 25 min. The maximum observed mixing ratio of CH_4 in the gas phase concentration was 77% at 150 m depth, which at this depth and thermal condition of the lake corresponds to 3.5 mmol L^{-1} . At deeper depth, dissolved CH_4 concentrations were too large for the methane absorption spectrum to be
20 correctly retrieved. Results were in good agreement with discrete in situ measurements conducted with the commercial HydroC sensor. The fast profiling feature will be highly profitable for future monitoring of the lake, while the spectrometer could be replaced with a less sensitive analytical technique possibly including simultaneous detection of dissolved CO_2 and which would allow to measure at higher concentrations of CH_4 .

1 Introduction

25 Lake Kivu is located in East Africa at the border between Rwanda and the Democratic Republic of the Congo. Its meromictic character, defined by a strong stratification of the water, makes deep water strongly decoupled from surface water because of their difference in density (Schmid and Wüest, 2012). The upper tens of meters (ranging from 65 to 25 m depending on seasons) correspond to the oxic zone, with life (fishes, algae and bacteria) while deeper waters are anoxic and contain large amount of dissolved carbon dioxide (CO_2) and methane (CH_4), with the strongest chemocline situated at 250 m of depth (Schmid
30 et al., 2005). Since 1935, several measurement campaigns have been carried out, aiming at quantifying the amount of dissolved



CH₄ and CO₂ present in the lake (e.g. (Degens et al., 1973; Pasche et al., 2011; Schmitz and Kufferath, 1955; Tassi et al., 2009; Tietze et al., 1980)). On the one hand, the presence of those gases constitute a risk of catastrophic event such as a gas eruption, which in the past already occurred in other gas-rich lakes (e.g. in 1984 at Lake Monoun and in 1986 at Lake Nyos in Cameroon (Kling et al., 1987; Kusakabe, 2017; Sigurdsson et al., 1987)). On the other hand, dissolved CH₄ represents a potentially important 35 energy resource. Already in 1963, the first on shore pilot plant started operations producing gas used by the Brewery BRALIRWA. In 2008, another off shore pilot plant was installed and could produce around 2 – 3 MW of electricity injected in the Rwandese national grid. In 2015, the first industrial power plant started with a capacity of 26 MW. Other plants are planned in the following years, not only for Rwanda but also for the Democratic Republic of the Congo. Methane extraction would allow to compensate further accumulation of gas at the bottom of the Lake and therefore preventing the possibility of a gas eruption. From this field 40 campaign, the maximum total dissolved gas pressure (TDGP) was estimated to be 50±7 % of the hydrostatic pressure at 320 m of depth (Bärenbold et al., 2019; Schmid et al., 2019). Meanwhile, extraction has to be performed without destabilizing the stratification of the lake or altering its ecosystem. Regarding the stability of the lake, in 2005 Schmid et al. (Schmid et al., 2005) raised the possibility that dissolved CH₄ in the lake was increasing with a rate of ~0.5 % per year, with consistent repercussion on the safety of the surrounding population. However, from the work of Pasche et al. (2011) as well as the results from this recent 45 field campaign, the hypothesis of a fast increase is today excluded, and the temporal variability appears to be slower than previously expected (Bärenbold et al., 2019; Boehrer et al., 2019; Schmid et al., 2019). In the future, regular monitoring of the lake is required for estimating the CH₄ and CO₂ budgets in the lake as well as their temporal variability, using reliable and easy to use techniques. For a more precise estimation of the dissolved gas content, inter-comparison between different sensors and methods is required, as conducted and presented in this work and in the even more comprehensive results from the entire inter- 50 comparison campaign (Bärenbold et al., 2019; Boehrer et al., 2019; Schmid et al., 2019).

The development of the Sub-Ocean sensor started as by-product from a development for measuring the composition of air bubble in-situ in ice sheets (Alemany et al., 2014; Grilli et al., 2014). After a first test in the Mediterranean Sea in 2014 with a different prototype but based on the same principle (Grilli et al., 2018), the sensor described and deployed here was developed. In October 2015 it was deployed over a hydrate degassing zone west of Svalbard, highlighting for the first time high variability 55 of dissolved CH₄ near the seabed together with a strong diffusivity most probably induced by the di-phasic medium generated by the gas flares (Jansson et al., 2019). In this work we report a successful deployment of the Sub-Ocean sensor in a very different setting, highlighting the reliability and adaptability of the technique to different aquatic environments. Advantages and drawbacks of the technique are highlighted in the discussion section. Two other research groups participated to the inter-comparison campaign using different methods: water sampling followed by laboratory gas chromatography analysis (Boehrer et al., 2019) 60 and on-line water pumping followed by on-site mass spectrometry analysis (Brennwald et al., 2016). These results are not reported here as they focused on the concentrations in the deep waters (Bärenbold et al., 2019; Schmid et al., 2019).



2 Materials and Methods

2.1 The Sub-Ocean MILS Instrument

The optical instrument used in this study is based on the OFCEAS technique (optical feedback cavity enhanced absorption spectroscopy) (Morville et al., 2003, 2014) developed for trace gas sensing. The dissolved air from the extraction unit (Figure 1) is continuously pumped toward the optical cavity of the spectrometer. The internal volume of the cell is less than 20 cm³ and provides sample residence times < 30 sec for optimal running conditions (compromise between the cell pressure and the total gas flow).

Extraction of dissolved gases from water is performed using a silicon rubber membrane. The extraction technique does not rely on gas equilibration across the membrane but, in order to achieve fast response, the dry side of the membrane is maintained at low pressure while continuously flushing it with dry zero air (Triest et al., 2017). The pressure at the membrane dry side controls the total flow of dry and wet air through the membrane, and the system is designed to keep this pressure constant. While the spectrometer operates at about 20 mbar, the pressure against the dry side of the membrane is maintained at about 30 mbar.

A full description of the in situ membrane inlet laser spectrometer (MILS) instrument, together with the experimental setup used for laboratory calibrations can be found in (Grilli et al., 2018). In order to adapt the instrument to the high concentrations of dissolved CH₄ expected in Lake Kivu, the absorption spectrum of the optical spectrometer was set away from the strong CH₄ rotational-vibrational transitions, more precisely at 2238.5 nm, where concentrations inside the optical cavity may reach up to 1.5 - 2 % of CH₄ in air before optical saturation (equivalent to an absorption 10⁻⁵ - 10⁻⁶ cm⁻¹). Above this absorption, the transmission signal at the maximum of the peak of absorption becomes too weak and the optical feedback to the laser, required with the OFCEAS optical technique, not strong enough to lock the laser frequency for a period of time close to the cavity free spectral range. This leads to narrower cavity modes and to a failure in retrieving the absorption feature correctly. In its standard setting, the membrane block (MB) is equipped with two semipermeable membranes allowing a large exchange surface with the water sample and therefore a large amount of gas that can permeate. For this campaign, one of the two membranes was replaced with a Teflon film. This increased the dilution factor by decreasing the flow of the permeating gas with respect to water vapour and the carrier gas flow, at the price of a degraded precision of the measurements due to the low dry gas flow thought the membrane. A picture of the instrument and the assembly taken during the campaign is reported in Figure 2. The main (central) pressure tube (140-cm long, 28-cm diameter) is mounted on a metal frame. The membrane block (MB) at the bottom is connected with a submersible water pump (Sea-Bird Electronics, SBE 5T) providing a flow of 0.8 L min⁻¹ along the membrane. A 1 L carrier gas (CG) tank containing dry zero air at a pressure between 2 and 40 bar depending on the suitable autonomy is attached on the frame and connected to the instrument via a 1/8" stainless-steel tube. A subsea battery (Seacell, STR) was mounted on the metal frame, providing up to 12 hours of continuous operation. An independent CTD (Sea & Sun Marine Tech, CTD-60) was also attached to the frame for depth, temperature, conductivity and dissolved oxygen measurements.



95

2.2 The HydroC-CH₄ commercial instrument

In situ discrete measurements of dissolved CH₄ at five different depths along the upper 150 m of the water column were performed using a commercial equilibrium-based underwater sensor, the HydroC HP system (Contros). The dissolved gas diffuses from the liquid through a thin film composite membrane into an internal gas cell. Therein, the total dissolved gas 100 pressure and the partial pressure of CH₄ gas are measured by a pressure sensor and a non-dispersive infrared spectrometer, respectively. The CH₄ sensor is similar to the HydroC-CO₂ sensor presented in (Fietzek et al., 2014), except for the absence of an internal zeroing system and a CH₄-specific fixed narrow-band spectral filter from 3.3–3.4 µm. The sensor was calibrated in October 2012 and November 2015 by the manufacturer. The calibrations were made using a specially designed pressure chamber with fresh water brought to pressure using compressed target gas. Three standard gas mixtures of CO₂, CH₄ and N₂ 105 (100 % pressure N₂; 50 % pressure CH₄ and 50 % pressure CO₂; 100 % pressure CH₄) were used to equilibrate the water volume along a gas pressure gradient (5–6 points) from 1 up to 30 bars and partial pressures of CH₄ from 0.5 to 18 bars. The calibration results showed the absence of a significant drift of the sensor (< 3 % within the Lake Kivu gas concentration range) between the October 2012 and November 2015 calibrations. Also, several CH₄ profiles were carried out in Lake Kivu from 2016 to 2018 using the HydroC CH₄-sensor and the repeatability of the observed CH₄ partial pressures was 3.8 % (2 σ) below 110 the main density gradient. However, the calibration curve as a function of the methane concentration was determined by using three points (0, 50 and 100% CH₄), and because of the nonlinear behavior of the detection system, a systematic error could be present, but it should not exceed 10 %.

The HydroC-CH₄ system was mounted on a SeaBird 19plus V2 SeaCAT CTD profiler equipped with a SBE 43 Dissolved Oxygen sensor and a SBE 18 pH sensor. Calibrations of the SeaBird sensors were performed following manufacturer 115 instructions. Water circulation in front of the HydroC membrane was provided by a SeaBird 5T pump, ensuring a continuous and homogeneous water flow to the membrane. A zero calibration of the HydroC-CH₄ system was made daily before each deployment using surface waters. The sampling rate was 1 Hz. The steady-state of the sensor was generally reached within 40 minutes and real-time data communication using an electromechanical cable allowed to adjust the waiting time at each depth accordingly. In all cases, the waiting time for each depth never exceeded 1 hour. The retained partial pressure of CH₄ is the 120 average for the last 5 min of the equilibration curve.

2.3 Calculation of dissolved CH₄

Both the MILS and the Hydro-C sensors measures CH₄ in the gas phase, and raw data are expressed as the concentration of CH₄ with respect to the total amount of dry gas permeating the membrane. For the MILS system, the concentration of CH₄ 125 in the dry gas downstream from the membrane [CH₄]_g' can be expressed with respect to the expected concentration of the gas in the headspace which would be in equilibrium with the water sample, [CH₄]_g. In eq. 1, Pr are the membrane permeability



coefficients for CH₄ and X (N₂, O₂ and CO₂) reported in Robb (1968), but corrected for their temperature and salinity dependency.

130
$$[CH_4]'_g = \frac{Pr_{CH_4} \cdot [CH_4]_g}{\sum Pr_X \cdot [X]_g} . \quad (1)$$

Concentrations, [CH₄], [X] are expressed as mixing ratios. Measuring the concentration of water vapor [H₂O]_g is required in order to retrieve the dissolved CH₄ concentration, [CH₄]_{dissolved}, since water vapor flow will cause dilution of the measured dry gas mixture (as well as the carrier gas flow). This measurement is performed by the OFCEAS spectrometer embedded in the
 135 Sub-ocean probe, simultaneously with the CH₄ measurement. Precision on the water vapor concentration was $\pm 0.6\%$ (2σ).
 [CH₄]_{dissolved} is then calculated from the following equation:

$$[CH_4]'_{dissolved} = \frac{[CH_4]'_g \times f_t}{f_t - f_{CG} - (f_t \times [H_2O]_g)} \times \frac{1}{m_{eff}} , \quad (2)$$

140 where [CH₄]_g' represents the methane mixing ratio measured by the optical spectrometer, f_t and f_{CG} are the total- and carrier-gas flow (ml min⁻¹), respectively, and [H₂O]_g corresponds to the mixing ratio of water permeating through the membrane. The denominator term ($f_t - f_{CG} - (f_t \times [H_2O]_g)$) corresponds to the dry flow permeating the membrane. m_{eff} represents the enrichment factor due to the membrane and corresponds to the quantity $\frac{Pr_{CH_4}}{\sum Pr_X \cdot [X]_g}$ in eq. 1. Its dependency with temperature and salinity is calculated by running calibrations under various conditions (Grilli et al., 2018). From our calibration, a m_{eff} of 2.84 ± 0.11 for
 145 fresh water at 25°C and 1.2 bar was calculated. This is in agreement with an expected value of 2.76 calculated from the permeation coefficients reported by Robb (1968).

As reported in eq. 1 above, this technique requires to know the main composition of the dissolved gas, in order to account for the different permeation coefficients of the species through the silicon membrane. This does not represent a problem for most of the ocean and lake settings, where the gas mixture is mainly composed of nitrogen and oxygen, but it requires a more
 150 complex analysis for a setting such as Lake Kivu. For the data analysis we assumed a bulk gas mainly composed of N₂, O₂, CO₂ and CH₄. H₂S is only present in bottom water and in lower amount with respect to CO₂ and CH₄, and was therefore neglected here. Oxygen concentrations were calculated from the CTD measurements and converted into partial pressure using equation 19 from Sander 2015 (using H^{cp} of 1.25×10^5 mol m⁻³ Pa⁻¹ and dln(H^{cp})/d(1/T) of 1500 K) (Sander, 2015).

As mentioned above, concentrations reported so far are expressed in mixing ratio with respect to the total dissolved gas
 155 pressure TDGP. Therefore, by knowing the TDGP, a value of partial pressure, pCH₄, can be retrieved which is then converted into dissolved methane concentrations, C_{CH₄}, expressed in mol per liter of water. This conversion is performed by taking into account the solubility of the gas in water under given physical conditions as well as its fugacity. The procedure has been previously described in a scientific report (Schmid et al., 2019). C_{CH₄} is related to the pCH₄ through the following equation:



160 $C_{CH_4} = K(T, S, P) p_{CH_4} \varphi_{CH_4}(T, P) ,$ (3)

where φ_{CH_4} is the fugacity coefficient, i.e. the ratio between the fugacity of a gas and its partial pressure, which is a function of temperature T , pressure P and gas composition, and K is the solubility coefficient, i.e. the ratio between the dissolved concentration of a gas and its fugacity. The solubility coefficient K (mol L⁻¹ atm⁻¹) of CH₄ as a function of temperature T (K) and salinity S (g/kg) is calculated using the following equation:

$$\ln(K) = A_1 + A_2(100/T) + A_3 \ln(T/100) + S[B_1 + B_2(T/100) + B_3(T/100)^2] , \quad (4)$$

The parameters in eq. 4 are from Wiesenburg and Guinasso (1979) (Wiesenburg and Guinasso, 1979).
170 The solubility coefficients need to be corrected for the local pressure P (bar) at the sampling depth (sum of hydrostatic pressure plus atmospheric pressure), using the following equation (Weiss, 1974):

$$K(P) = K e^{\left[\frac{(1-P) v_{CH_4}}{RT} \right]} , \quad (5)$$

where $R = 83.1446 \text{ cm}^3 \text{ bar K}^{-1} \text{ mol}^{-1}$ is the gas constant, and v_{CH_4} is the partial molar volume (cm³ mol⁻¹) of CH₄ calculated from Rettich et al., 1981 (Rettich et al., 1981).
175 The fugacity coefficients were calculated using the methods described by Ziabakhsh-Ganji and Kooi (Ziabakhsh-Ganji and Kooi, 2012). A Maple script was provided by Z. Ziabakhsh-Ganji, which was transcribed to Matlab code by M. Schmid (Schmid et al., 2019). The script calculates, among other things, the fugacity coefficients for CO₂ and CH₄, including the interactions between both gases.

180 **2.4 The Lake and the field campaign**

Lake Kivu [2.50°S - 1.59°S ; 29.37°E - 28.83°E] located at 1460 m above sea level, has a surface of 2 700 km² (of which 2385 km² represents the water covering) and a maximum depth of ~485 m. The measurement campaign took place from 9th to 13th March 2018 at ~6 km from Goma and ~5 km from Gisenyi/Rubavu at the Northern shore of the lake (1.74087°S - 29.22602°E) and nearby a permanent platform with water depth of 410 m. During the campaign other type of measurements of dissolved methane and carbon dioxide were performed. The research team from Eawag (Switzerland) analyzed pumped water on the platform using a field mass spectrometer instrument (Brennwald et al., 2016), while a second team from UFZ (Germany) sampled water from a boat and measured the samples by head-space equilibration and gas chromatography (GC) analysis at the Lake Kivu Monitoring Program (LKMP) laboratory in Rubavu (Boehrer et al., 2019). The Sub-Ocean sensor was deployed from a research boat during three days of the campaign: 10th, 12th and 13th of March, with a total of eight continuous profiles.



190 Measurements with the commercial Hydro-C sensor were conducted during the campaign and on May 8th -11th at the same location than the Sub-Ocean measurements.

3 Results

In Figure 4 an example of a consecutive downward and upward profile of dissolved CH₄ measured by the Sub-Ocean sensor is reported. CH₄ concentrations are expressed as mixing ratio with respect to the total dissolved gas. The sensor was 195 lowered at a speed of ~6 m/min, reaching 100 m depth in only 18 min. The response time of the sensor during the campaign expressed as τ_{90} was ~10 sec, which corresponds to a vertical resolution of 1 m. On the right-hand side, dissolved CH₄ is plotted against depth, showing the reproducibility of the sensor during descent and ascent.

A total of eight continuous profiles (downward and upward) were obtained with the Sub-ocean instrument during the campaign. They are reported in Figure 5 together with dissolved CO₂, CTD data (temperature, conductivity and dissolved 200 oxygen) and total dissolved gas pressure (TDGP). For the measurement of CH₄ only one of the eight profiles reached 150 m, while the others are shallower, only covering the upper 100 m of depth. The accuracy of the measurement was estimated at 80 m depth, where water mass is well stratified. At this depth, an average concentration of $35.5 \pm 7.8\%$, corresponding to 508.3 ± 112 mbar of partial pressure and 0.71 ± 0.16 mmol L⁻¹ of CH₄ was calculated, leading to a repeatability of $\pm 22\%$ (2σ). This 205 relatively large standard deviation can be explained by the large uncertainty in retrieving the flow of dry gas permeating the membrane. The value is in agreement with previously observed performances, where an error propagation of $\pm 12\%$ (2σ) was calculated using two semipermeable membranes (Grilli et al., 2018). The use of only one membrane allowed to further increase the dynamic range of the sensor by playing on the dilution factor applied on the dry gas permeating the membrane. However, in this condition, a dry gas flow of only ~ 0.065 cm³ STP/min is delivered by the extraction system. The large uncertainty on 210 this dry flow measurement directly affects the accuracy on the retrieved concentration. The $\pm 22\%$ error was therefore used as the uncertainty of the average continuous profile. The CO₂ data are from Schmid et al. (2005) and are calculated from alkalinity and pH measurements (Schmid et al., 2005). TDGP are discrete measurements at seven different depths measured with the HydroC sensor which have been interpolated to match the depth resolution of the Sub-ocean data. Nitrogen, N₂, mixing ratio was retrieved assuming that the main gas is composed by N₂, CO₂, CH₄, and O₂ ($pN_2 = TDGP - pCH_4 - pCO_2 - pO_2$). The molar concentrations as a function of depth for the average continuous profile recorded by the Sub-Ocean sensor and for 215 the discrete measurements obtained with the HydroC sensor are reported in Figure 6. A good agreement between the two independent measurements is observed. The measurements were obtained during the same field campaign at the measurement site location near Goma (the two vessels were a few hundred meters away from each other). However, the measurements were not performed simultaneously. In the graph, results from previous campaigns are also reported. Data from the University of Liege obtained during a long term monitoring of the lake are reported in orange. Data were collected from June 2011 to August 220 2014 at different periods of the year (both dry and rainy seasons) and at different locations (northern and south basin) (Roland et al., 2017, 2018). The large variability of these data is reported by the orange lines defining the 3σ distribution of the data.



Data from the works of Pasche et al. 2011 and Schmid et al. 2005 are also reported in green and blue, respectively. Data from ULiege and Pasche 2011 were obtained by sampling the water using Niskin bottles and analyzing the dissolved gas in the laboratory by head-space technique. The others (this work and Schmid 2005) are from in situ measurements. From the data,

225 one can see that below 80 m depth, where the TDGP becomes larger than atmospheric pressure (1.4 bar at 80 m, Figure 5), a problem due to degassing of the sample collected on the Niskin bottles was observed, leading to an under-estimation of the dissolved CH₄. Data from Schmid 2005, which are from a commercial Capsum Met sensor (Franatech) and data from the Contros sensor are a bit lower than the measurements with the Sub-Ocean probe at higher concentrations (and depths), but they still lie within the measurement uncertainties. For the same campaign, the Contros sensor dataset at larger depths (> 150m)

230 also sits at lower values of dissolved methane with respect to the other two measurement techniques. (Schmid et al., 2019). This may be due to a problem of calibration of the sensor, but it definitely requires a further investigations. Regarding the Capsum Met sensor, no information about the calibration of the sensor were found, therefore not further discussion can be carried out.

Surface measurements performed by the Sub-Ocean instrument lead to average concentrations of $0.59 \pm 0.03 \mu\text{mol L}^{-1}$ and 235 $0.72 \pm 0.14 \mu\text{mol L}^{-1}$ over the upper 10 and 30 m, respectively. Those values sit at the higher edge of the observed average seasonal concentrations, which span from 0.008 to $11 \mu\text{mol L}^{-1}$ (Roland et al., 2017, 2018, and more recent unpublished data).

Despite the large seasonal and spatial variability, our results are in good agreement with the one from Pasche et al 2011 which were obtained at a similar time of the year but at different locations (May 2006 and 2007 in Kibuye, Gisenyi and Ishungu). A stronger similarity can be found with the dataset from the same location (Gisenyi 2007) in the northern basin. CTD 240 measurements (temperature, conductivity and dissolved oxygen, Sea & Sun Marine Tech, CTD-90M) performed a few months prior to the campaign at the research platform (Figure 7) confirmed a typical behavior of the lake stratigraphy while going from a dry into a rainy season (Roland et al., 2017). The lake was mixed down to at least 50 m depth during the previous dry season, and started to stratify in mid-December, leading to a 25-m depth seasonal thermocline. Below the thermocline, O₂ was rapidly consumed by mineralisation of organic matter and oxidation of reduced compounds (eg. methane, ammonium) 245 diffusing upward. By the end of February, O₂ supplied at these depths during the previous dry season was completely vanished.

Then, on the first-half of March, a mixing event occurred down to about 35 m depth, favoring the mixing between anoxic water (35-25 m depth), enriched in dissolved CH₄, and surface water. From the top 10 m layer temperature profiles reported in Figure 7 one can see that by March 22nd the temperature slope disappeared, supporting the occurrence of the mixing event.

Unfortunately, the reason for this mixing event are still unknown. Meteorological records from December 2017 to March 2018 250 do not indicate neither high wind speed, low temperature, nor low relative humidity events that could clearly support our observations. Comparing the second half of February to the first half of March, average temperatures decreased by 1°C (from 21.2 to 22.2°C) and average precipitations increased by a factor of two, with peaks up to 7.6 mm of rainfall on March 6th. As reported by Rooney et al., 2018, rain may have a cooling effect on the lake surface by lowering the near-surface air temperature and inducing a convective mixing of the lake surface layer. Further investigations are required for better understanding the 255 dynamic of the surface layer of the lake at this period of the year.



4 Discussion and Conclusions

The comparison between different types of measurements highlights the reliability of the fast response membrane extraction system that is integrated in the Sub-Ocean sensor under more extreme conditions (in terms of dissolved gas content) than ocean settings. Lake Kivu is particularly challenging because of the high amount of dissolved CH₄ and CO₂ as well as 260 their large variability. The gas composition strongly varies across the oxic-anoxic boundary and further down across the different chemoclines, going from a background composed by N₂ and O₂, to another one which sees CH₄ and CO₂ as the main dissolved gases. The Sub-Ocean sensor allowed fast vertical profiles of CH₄ which are in good agreement with the discrete in situ measurements made with the commercial HydroC sensor at five different depths. At 80 m of depth, not spatial variability 265 of the dissolved gas is expected and we therefore estimate the accuracy of the SubOcean sensor to $\pm 22\%$ (2σ) by comparing the eight independent profiles at this depth. The maximum measurable concentration of dissolved CH₄ was 3.5 mmol L⁻¹ at 24°C, 150 m of depth, and TDGP of 2.62 bar, which corresponds to a mixing ratio of 77% with respect to the total dissolved gas.

An average concentration of $0.59 \pm 0.03 \mu\text{mol L}^{-1}$ of CH₄ was founded in the 10-m surface layer, which sits at the higher edge of the observed average seasonal concentrations of the lake. In the result section, the possible reasons for this have been 270 discussed. The variability of the physical parameters during a period of three months prior the campaign suggest a mixing event of the top 35 m, but the causes are not yet clear and further investigations will be required for better understating the behavior of the lake while going from the dry into the rainy season.

Such a campaign highlights the advantages of using the Sub-Ocean technology for measuring the dissolved gas content in meromictic lake settings. The technology allows in situ, continuous and fast profiling, important for a long term monitoring 275 of water resources. The in situ deployment allows to avoid any possible contamination and artefact of the measurement due to water and/or gas sampling and subsequent laboratory analyses. The fast response of the instrument would allow to complete a full vertical profile over 470 m of depth within $\sim 1\text{h } 20\text{min}$ while current techniques of in situ discrete sampling would take 1h per measured depth. The measurement by this technique has now been proven over a very large dynamic range of seven orders 280 of magnitude, spanning from sub-nmol L⁻¹ in open ocean waters to mmol L⁻¹ concentrations of dissolved CH₄ and in a context of very different dissolved gas composition and TDGP.

Beside those advantages, some drawbacks can be identified: **i)** the instrument was designed for measuring background concentrations in the oceans (sub-nmol L⁻¹) while Lake Kivu reaches $\sim 18 \text{ mmol L}^{-1}$ in bottom waters, thus with an eight orders of magnitude difference. For the campaign, the spectrometer sensitivity was reduced by tuning the laser frequency to a region where weaker methane absorption bands could be found. Further, the dilution factor of the extraction system was maximized 285 by removing one of the two silicon membranes and by increasing the carrier gas flow to its maximum allowed by the vacuum system embedded in the sensor. Despite those efforts, Sub-Ocean could not measure below 150 m depth, corresponding to a maximum measurable concentration of 3.5 mmol L⁻¹, where absorption becomes too strong for the optical spectrometer at the selected laser frequency. **ii)** In such environment, a good knowledge of the total dissolved gas pressure and of the concentration



of dissolved CO₂ are required for a correct retrieving of the concentration of CH₄. Those parameters were measured during the
290 field campaign, but they are not currently integrated in the sensor. This could be performed in the future by detecting simultaneously CO₂ and CH₄ using the same gas analyzer and by integrating the TDGP measurement or deploying the sensor with an independent TDGP device. It should be noticed that TDGP sensors have response times of a few minutes (e.g. $\tau_{63} = 2$ min for the Mini-TDGP from Pro-Oceanus) which could be a limiting factor with respect to the faster response time of the Sub-Ocean sensor. **iii)** Because a low dry gas flow was required (in order to increase the dilution factor), the precision of the
295 measurement was degraded by a factor of two with respect to previous deployments, leading to a $\pm 22\%$ precision. By using a less sensitive gas analyzer, the above drawbacks could be avoided, or at least minimized, making the technique fully suitable for monitoring meromictic lakes within a large range of dissolved CH₄ concentration.

Author Contributions: RG, JT and JC are the inventors of the Sub-Ocean instrument. JC, AM and AU initiated the
300 collaboration leading to the field campaign. AM and AU organized the field campaign and took care of the project administration. RG optimized the instrument for the measurements at Lake Kivu and ran the laboratory calibration. RG prepared the instrument for the field and was in charge of the field campaign with the Sub-Ocean instrument. FD handled the measurements with the HydroC sensor and its data analysis. JT contributed to the analysis of the HydroC sensor and TDGP. RG analyzed the Sub-Ocean data. All authors contributed to the manuscript.

305

Funding: This research was funded by the European Community's Seventh Framework Programme ERC-2015-PoC, grant number 713619 (ERC OCEAN-IDs), the European Community's Seventh Framework Programme ERC-2011-AdG, grant number 291062 (ERC ICE&LASERS) and the National Research Funding, ANR, through the program ANR-18-CE04-0003-01.

310

Acknowledgments: The research leading to these results has received funding from the European Community's Seventh Framework Programme ERC-2015-PoC under grant agreement no. 713619 (ERC OCEAN-IDs). The work was made possible thanks to pioneering investigations conducted under the European Community's Seventh Framework Programme ERC-2011-AdG under grant agreement no. 291062 (ERC ICE&LASERS) and with support from SATT Linksum of Grenoble, France,
315 and of the Service Partenariat & Valorisation (SPV) of the CNRS. The authors would like to thank Martin Schmid for his profitable help and discussions regarding the conversion from partial pressure into concentration units. Fabian Bärenbold, Bertram Boehrer, Wolf von Tümpeling, Placid Nkusi, Maximilian Schmidt, Eric Mudakikwa, Irénée Nizere, Gaeta Sakindi, the captain of the vessel for their help during the field campaign and their helpful discussions. Thanks to the entire Lake Kivu Monitoring Program for the organization of the field campaign. We thanks Wim Thiery and Nicole van Lipzig for providing
320 the meteorological data. We also thanks Alberto Borges and Fleur Roland and Martin Schmid for the discussions on the surface water mixing. Véronique Gosselain (University of Louvain, Belgium) is thanked for her networking to put the Lake Kivu Monitoring Program and scientists from IGE, Grenoble, France, in connection.



Conflicts of Interest: The authors declare no conflict of interest.

325 **References**

Alemany, O., Chappellaz, J., Triest, J., Calzas, M., Cattani, O., Chemin, J. F., Desbois, Q., Desbois, T., Duphil, R., Falourd, S., Grilli, R., Guillerme, C., Kerstel, E., Laurent, B., Lefebvre, E., Marrocco, N., Pascual, O., Piard, L., Possenti, P., Romanini, D., Thiebault, V. and Yamani, R.: The SUBGLACIOR drilling probe: concept and design, *Ann. Glaciol.*, 55(68), 233–242, doi:10.3189/2014AoG68A026, 2014.

330 Bärenbold, F., Boehrer, B., Grilli, R., Mugisha, A., Tümping, W. von, Umutoni, A. and Schmid, M.: Updated dissolved gas concentrations in Lake Kivu from an intercomparison project, *Prep.*, 2019.

Boehrer, B., von Tümping, W., Mugisha, A., Rogemont, C. and Umutoni, A.: Reliable reference for the methane concentrations in Lake Kivu at the beginning of industrial exploitation, *Hydrol. Earth Syst. Sci. Discuss.*, 1–26, doi:10.5194/hess-2019-228, 2019.

335 Brennwald, M. S., Schmidt, M., Oser, J. and Kipfer, R.: A Portable and Autonomous Mass Spectrometric System for On-Site Environmental Gas Analysis, *Environ. Sci. Technol.*, 50, 13455–13463, doi:10.1021/acs.est.6b03669, 2016.

Degens, E. T., von Herzen, R. P., Wong, H., Deuser, W. G., Jannasch, H. W. and Hole, W.: Lake Kivu : Structure , Chemistry and Biology of an East African Rift Lake, *Geol. Rundschau*, 62(1), 245–277, 1973.

340 Encinas Fernández, J., Peeters, F. and Hofmann, H.: Importance of the autumn overturn and anoxic conditions in the hypolimnion for the annual methane emissions from a temperate lake, *Environ. Sci. Technol.*, 48(13), 7297–7304, doi:10.1021/es4056164, 2014.

Fietzek, P., Fiedler, B., Steinhoff, T. and Körtzinger, A.: In situ Quality Assessment of a Novel Underwater pCO₂ Sensor Based on Membrane Equilibration and NDIR Spectrometry, *J. Atmos. Ocean. Technol.*, 31, 181–196, doi:10.1175/JTECH-D-13-00083.1, 2014.

345 Grilli, R., Marrocco, N., Desbois, T., Guillerm, C., Triest, J., Kerstel, E. and Romanini, D.: Invited Article : SUBGLACIOR : An optical analyzer embedded in an Antarctic ice probe for exploring the past climate, *Rev. Sci. Instrum.*, 85(111301), 1–8, doi:10.1063/1.4901018, 2014.

Grilli, R., Triest, J., Chappellaz, J., Calzas, M., Desbois, T., Jansson, P., Guillerm, C., Ferré, B., Lechevallier, L., Ledoux, V. and Romanini, D.: Sub-Ocean: subsea dissolved methane measurements using an embedded laser spectrometer technology, *Environ. Sci. Technol.*, 52, 10543–10551, doi:10.1021/acs.est.7b06171, 2018.

350 Jansson, P., J., T., Grilli, R., Ferré, B., Silyakova, A., Mienert, J. and Chappellaz, J.: High-resolution under-water laser spectrometer sensing provides new insights to methane distribution at an Arctic seepage site, *Ocean Sci.*, 15, 1055–1069, doi:10.5194/os-15-1055-2019, 2019.

Kling, G. W., Clark, M. A., Compton, H. R., Devinee, J. D., Evans, W. C., Humphrey, A. M., Koenigsberg, E. J., Lockwood,



355 J. P., Tuttle, M. L. and Wagner, G. N.: The 1986 Lake Nyos Gas Disaster in Cameroon , West Africa, *Science* (80-.), 236, 169–175, doi:10.1126/science.236.4798.169, 1987.

Kusakabe, M.: Lakes Nyos and Monoun Gas Disasters (Cameroon)—Limnic Eruptions Caused by Excessive Accumulation of Magmatic CO₂ in Crater Lakes, *GEOchemistry Monogr. Ser.*, 1(1), 1–50, doi:10.5047/gems.2017.00101.0001, 2017.

Morville, J., Romanini, D. and Chenevier, M.: WO03031949, (Université J. Fourier, Grenoble FRANCE, 2003), 2003.

360 Morville, J., Romanini, D. and Kerstel, E.: Cavity Enhanced Absorption Spectroscopy with Optical Feedback, in *Cavity-Enhanced Spectroscopy and Sensing*, edited by G. Gagliardi and H.-P. Loock, pp. 163–209, Springer Berlin Heidelberg., 2014.

Pasche, N., Schmid, M., Vazquez, F., Schubert, C. J., Wüest, A., Kessler, J. D., Pack, M. A., Reeburgh, W. S. and Bürgmann, H.: Methane sources and sinks in Lake Kivu, *J. Geophys. Res. Biogeosciences*, 116(3), 1–16, doi:10.1029/2011JG001690, 2011.

365 Rettich, T. R., Handa, Y. P., Battino, R. and Wilhelm, E.: Solubility of gases in liquids. 13. High-precision determination of Henry's constants for methane and ethane in liquid water at 275 to 328 K, *J. Phys. Chem.*, 85(22), 3230–3237, 1981.

Robb, W. L.: Thin silicon membranes. Their permeation properties and some applications, *Ann. N. Y. Acad. Sci.*, 146, 119–137, doi:10.1111/j.1749-6632.1968.tb20277.x, 1968.

Roland, F. A. E., Darchambeau, F., Morana, C. and Borges, A. V.: Nitrous oxide and methane seasonal variability in the 370 epilimnion of a large tropical meromictic lake (Lake Kivu, East-Africa), *Aquat. Sci.*, 79(2), 209–218, doi:10.1007/s00027-016-0491-2, 2017.

Roland, F. A. E., Morana, C., Darchambeau, F., Crowe, S. A., Thamdrup, B., Descy, J. P. and Borges, A. V.: Anaerobic methane oxidation and aerobic methane production in an east African great lake (Lake Kivu), *J. Great Lakes Res.*, 44(6), 1183–1193, doi:10.1016/j.jglr.2018.04.003, 2018.

375 Rooney, G. G., Van Lipzig, N. and Thiery, W.: Estimating the effect of rainfall on the surface temperature of a tropical lake, *Hydrol. Earth Syst. Sci.*, 22(12), 6357–6369, doi:10.5194/hess-22-6357-2018, 2018.

Sander, R.: Compilation of Henry 's law constants (version 4.0) for water as solvent, *Atmos. Chem. Phys.*, 15, 4399–4981, doi:10.5194/acp-15-4399-2015, 2015.

Schmid, M. and Wüest, A.: Stratification, Mixing and Transport Processes in Lake Kivu, in *Lake Kivu: Limnology and 380 biogeochemistry of a tropical great lake*, Springer Science+Business Media B.V. 2012., 2012.

Schmid, M., Halbwachs, M., Wehrli, B. and Wuest, A.: Weak mixing in Lake Kivu: New insights indicate increasing risk of uncontrolled gas eruption, *Geochemistry Geophys. Geosystems*, 6(7), 1–11, doi:10.1029/2004GC000892, 2005.

Schmid, M., Bärenbold, F., Boehrer, B., Darchambeau, F., Grilli, R., Triest, J. and Von Tümpeling, W.: Intercalibration Campaign Measurements in Lake Kivu for Gas Concentration. Report prepared for the Lake Kivu Monitoring Programme 385 (LKMP) of the Energy Development Corporation Limited (EDCL), Kigali, Rwanda., 2019.

Schmitz, D. and Kufferath, J.: Problèmes posés par la présence de gaz dissous dans les eaux profondes du Lac Kivu, *Acad Roy Sci Colon. Bull Séances*, 1, 326–356, 1955.

Sigurdsson, H., Devine, J. D., Tchoua, F. M., Presser, T. S., Pringle, M. K. W. and Evans, W. C.: Origin of the lethal gas burst



from Lake Monoun, Cameroon, *J. Volcanol. Geotherm. Res.*, 31(March 1985), 1–16, 1987.

390 Tassi, F., Vaselli, O., Tedesco, D., Montegrossi, G., Darrah, T., Cuoco, E., Mapendano, M. Y., Poreda, R. and Delgado Huertas, A.: Water and gas chemistry at Lake Kivu (DRC): Geochemical evidence of vertical and horizontal heterogeneities in a multibasin structure, *Geochem. Geophys. Geosyst.*, (10), doi:10.1029/2008GC002191, 2009.

Tietze, K., Geyh, M., Müller, H. and Schröder, L.: The Genesis of the Methane in Lake Kivu (Central Africa), *Geol. Rundschau*, (69), 452–472, 1980.

395 Triest, J., Chappelaz, J. and Grilli, R.: Patent 08276-01: System for fast and in-situ sampling of dissolved gases in the ocean (CNRS, Grenoble FRANCE), 2017.

Weiss, R. F.: Carbon dioxide in water and seawater: the solubility of a non-ideal gas, *Mar. Chem.*, 2(3), 203–215, doi:10.1016/0304-4203(74)90015-2, 1974.

Wiesenburg, D. A. and Guinasso, N. L.: Equilibrium solubilities of methane, carbon monoxide, and hydrogen in water and sea

400 water, *J. Chem. Eng. Data*, 24(4), 356–360, doi:10.1021/je60083a006, 1979.

Ziabakhsh-Ganji, Z. and Kooi, H.: An Equation of State for thermodynamic equilibrium of gas mixtures and brines to allow simulation of the effects of impurities in subsurface CO₂storage, *Int. J. Greenh. Gas Control*, 11S, S21–S34, doi:10.1016/j.ijggc.2012.07.025, 2012.

405

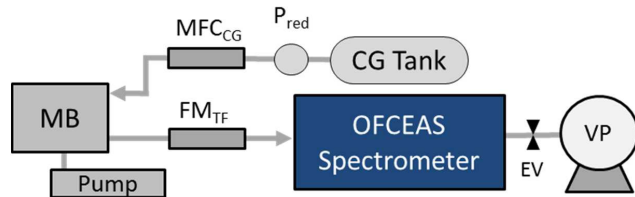
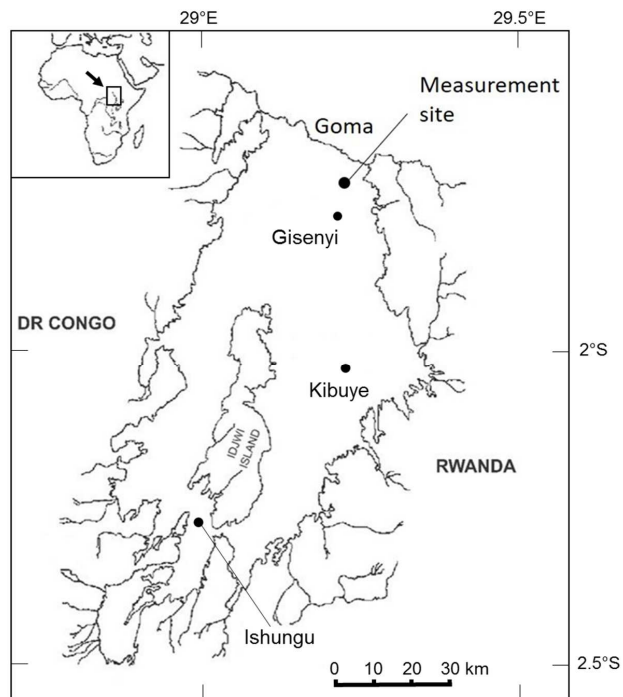


Figure 1. A schematic of the Sub-Ocean Sensor. MB is the membrane block where the gas extraction occurs. Water circulates against the membrane using a submersible pump. The carrier gas (CG) flow is controlled by a mass flow controller (MFC_{CG}) and the flowmeter FM_{TF} is used for monitoring the total gas flow. The low pressure on the optical spectrometer is provided by a vacuum pump (VP) and an electronic valve (EV). P_{red} is a pressure reducer.



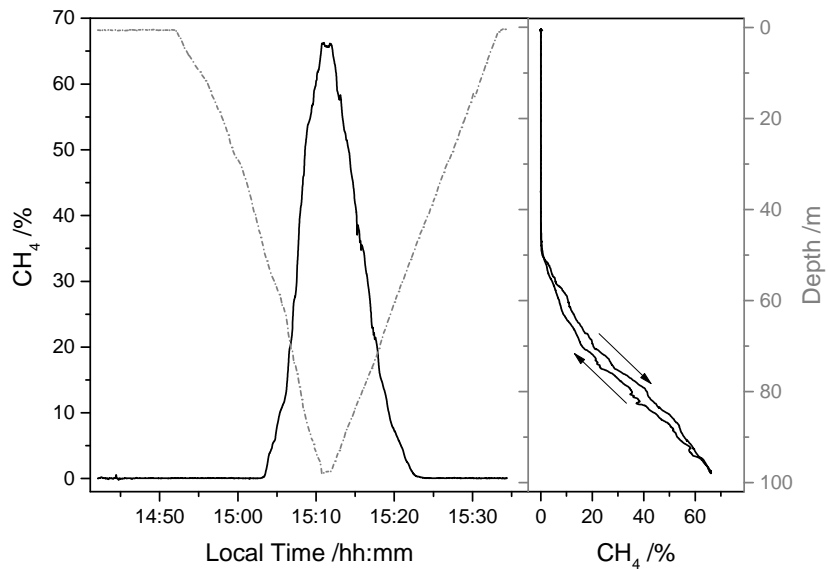
Figure 2. A picture of the Sub-Ocean instrument and the full assembly. The sensor is mounted on a metal frame. The main tube at the center is 150-cm long and 28-cm diameter. The membrane block (MB) at its bottom is connected to the water pump to ensure a constant flow of water against the membrane. The carrier gas (CG) tank is attached to the metal frame and connected with a 1/8" stainless-steel tube at the instrument. An STR battery pack and a CTD sensor were also attached to the metal structure. The total weight of the assembly is 120 kg with about -50 kg of buoyancy.

415



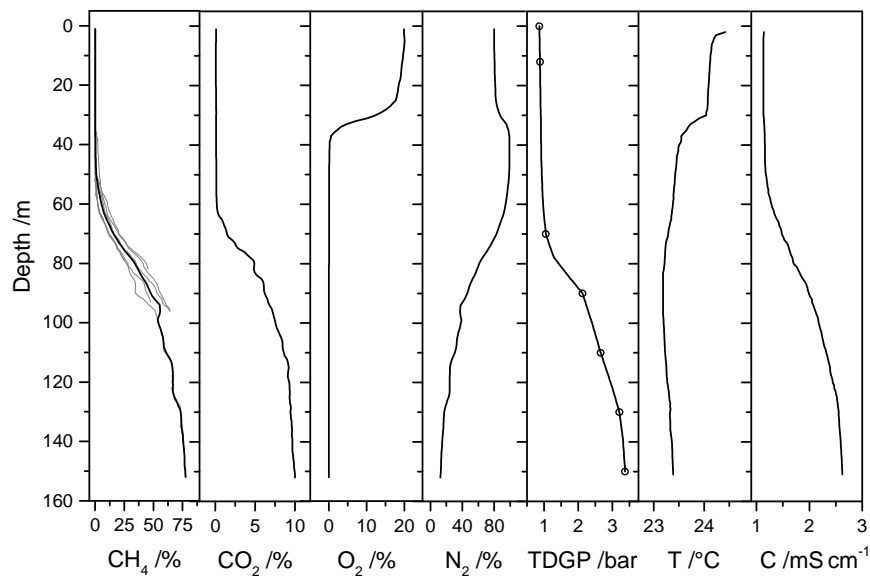
420

Figure 3. Map of Lake Kivu showing the location of the measurement site. Locations of previous campaigns mentioned in the discussion part are also reported (named Gisenyi, Kibuye and Ishungu).



425

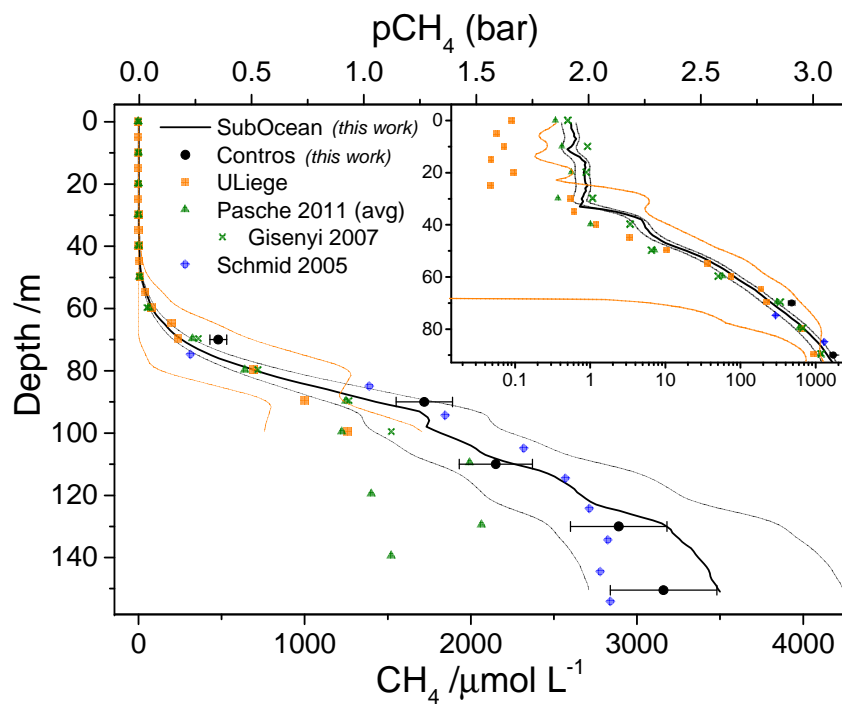
Figure 4. One of the methane continuous profiles recorded by the Sub-Ocean on 10th March 2018. The concentration is expressed as a percentage of CH₄ with respect to the total dissolved gas. The 100 m downward and upward profile was recorded in 42 min. On the right panel the two profiles are superposed, highlighting the reproducibility of the measurement between descent and ascent.



430

435

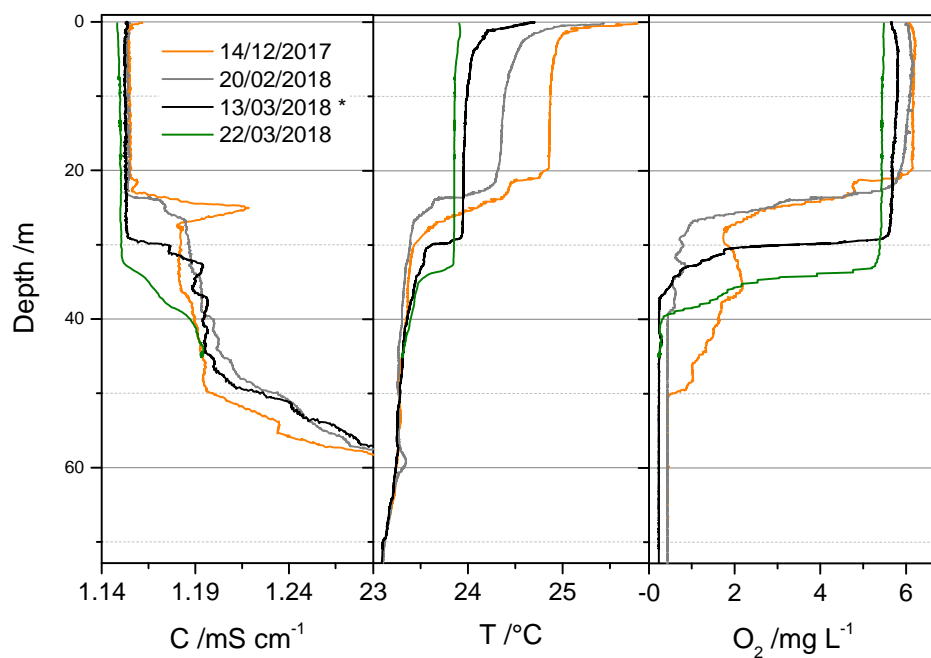
Figure 5. Mixing ratios of individual gas species in the dissolved gas mixture and total dissolved gas pressure. Grey CH_4 lines combine the eight profiles recorded by the Sub-Ocean instrument during the campaign, while the black line is the averaged value. CO_2 data are from (Schmid et al., 2005), O_2 comes from CTD data during the campaign, and N_2 is a retrieved concentration profile deduced from the other measurements ($\text{TDGP} = p\text{CH}_4 + p\text{CO}_2 + p\text{O}_2$). The total dissolved gas pressure, TDGP, was measured using the Contros HydroC sensors (open circles), the black line is an interpolation of the data. Temperature and electrical conductivity were recorded by the CTD during the deployment.



440

Figure 6. Continuous methane profile of the upper 150 m of water depth in Lake Kivu measured by the Sub-Ocean instrument (black line) with the corresponding estimated uncertainty of $\pm 22\%$ (grey lines). Concentrations are plotted against depth. Black dots are discrete measurements made with the Contros Hydro-C sensor at different depths. Error bars corresponds to the estimated uncertainty of $\pm 10\%$. Orange squares are from the long term monitoring from the University of Liege (Roland et al., 2017, 2018) with the corresponding 3σ variability (orange lines). Green triangles are average concentrations from Pasche et al. 2011 (Pasche et al., 2011) from three different campaigns conducted in May 2006 and 2007 at different locations (Kibuye, Ishungu and Gisenyi). Green crosses are data from Gisenyi 2007. Blue rhombus correspond to measurements from Schmid et al. 2005 in the northern basin using a commercial Capsum Met sensor (Schmid et al., 2005).

445



450 **Figure 7.** CTD (conductivity at 25°C, temperature and dissolved oxygen) data obtained a few months prior to the campaign. The black lines correspond to the conditions during the field measurements (*). The O₂ profiles highlight how the mixing layer extended down to 50 m depth during the previous dry season. From mid-December, the lake started to stratify at 25 m, while at the beginning of March the oxic layer increased down to 35 m depth.